Journal of Energy Research and Reviews

9(1): 51-66, 2021; Article no.JENRR.75258
ISSN: 2581-8368

Study of the Behavior of Air Parcels, Using PIXE, Hysplit and Wind Rose in the Metropolitan Zone of Toluca Valley, Mexico

Angélica Flores Ortiz[1], María de la Luz Jiménez Núñez[1] and Raúl Venancio Díaz Godoy[2*]

[1]TecNM/Technological Institute of Toluca (ITTol), State of Mexico, Mexico.
[2]National Institute for Nuclear Research (ININ), State of Mexico, Mexico.

Authors' contributions

This work was carried out in collaboration among all authors. All authors read and approved the final manuscript.

Article Information

DOI: 10.9734/JENRR/2021/v9i130225
Editor(s):
(1) Dr. Davide Astiaso Garcia, Sapienza University of Rome, Italy.
Reviewers:
(1) Hilario Becerril Hernandez, Colegio de Postgraduados, Mexico.
1. (2) Bankole Adebanji, Ekiti State University, Nigeria.
Complete Peer review History: http://www.sdiarticle4.com/review-history/75258

Original Research Article

Received 14 August 2021
Accepted 29 October 2021
Published 03 November 2021

ABSTRACT

Aim: The objective of this work was to determine the behavior of the trajectories of the air plots in two sites (San Mateo Atenco-(SM) and San Lorenzo Tepaltitlán-(SL)), in the atmosphere of the Metropolitan Zone of the Toluca Valley (MZTV).
Methodology: In the atmosphere of the MZTV, using HYSPLIT a Backward trajectory direction analysis was performed from June 29 to July 8, 2021, considering for each day the summertime schedules of the center, indicating its Coordinated Universal Time (UTC). An ANOVA analysis (with a significance level of α=0.05) was performed for the concentrations of SM and SL obtained with PIXE, with the objective of seeing the equality of their behavior.
Results: The behavior of the direction of the trajectories of the air plots in both sites is similar and the trajectories for the same day are the same in both sites but different on another day; It was determined that during night-day (19 to 12 h of the following day) the behavior is similar and changes during the remaining time, being variable. In general, the origin of the trajectories of the air plots for both sites of the MZTV is predominantly from the southeast, a situation that was confirmed with Wind Roses. Of the ANOVA analysis, the p-value was in all cases greater than the significance

**Corresponding author: E-mail: rvdginin2011@gmail.com;*

level of 0.05, the null hypothesis was accept, and it is possible to conclude that the elemental chemical composition of $PM_{2.5}$ have equal means in both sites.
Conclusion: Among other, it is possible to consider the behavior of meteorological parameters and thus take them into account for sampling studies of criteria pollutants such as $PM_{2.5.}$

Keywords: PIXE; Hysplit; trajectories; wind roses; sources; $PM_{2.5}$; MZTV; accelerators.

1. INTRODUCTION

Within the framework of energy, we have atomic-nuclear energy, in which the PIXE (Proton Induced X-Ray Emission) technique is used, which uses as a fundamental tool for its application, a particle accelerator with which the collision of nuclei with projectiles is carried out [1,2]. In this work, taking advantage of the results obtained with this and the Hysplit modeling technique as well as the Wind Roses, it will be possible to know the emission sources of pollutants and their behavior.

Atmospheric pollution in the world is becoming more alarming every day due to the number of diseases and deaths it causes every year. Our country is not the exception and most of the states of the republic present serious episodes of pollution that requires studies to characterize it, which entails the need to know the emission sources that produce it, several researchers have studied this origin.

In their study *Emission inventory point source visualization on Google Earth and integrated with HYSPLIT model*, used Google Earth to couple the data of a point source with a hypothetical release for that source, simulated with the Hybrid Single Particle Lagrangian Integrated Trajectory Model (HYSPLIT) developed by the National Oceanic and Atmospheric Administration (NOAA). This work shows that Google Earth or any smartphone application that reads and displays KML data files allows visualization of the point source location, and its emission puff releases or trajectories. In addition, it works for air quality management, querying and receiving information for any source assessment and could include data from atmospheric surveillance networks and air quality monitoring sites [3].

In the study Analysis of a Severe $PM_{2.5}$ Episode in the Seoul Metropolitan Area in South Korea from 27 February to 7 March 2019: Focused on Estimation of Domestic and Foreign Contribution, they conducted a backward-trajectory analysis using the HYSPLIT model to analyze the origin of the air mass that moved toward the metropolitan area, to the monitoring stations, of Seoul during the severe $PM_{2.5}$ episode. The results of the analysis showed that the air mass moved into Seoul through the eastern and northern parts of China and the Liaodong Peninsula during the P1 period. Atmospheric stagnation and wind deflection occurred during the P2 period, and air from around Beijing and the Shandong Peninsula moved into Seoul during the P3 period. During the P4 period, when the concentration of $PM_{2.5}$ decreased, northerly winds were introduced into South Korea [4].

The Mario Molina Center conducted the analysis of $PM_{2.5}$ pollution in the city of Monterrey, Nuevo Leon, focused on the identification of strategic control measures, developed modeling exercises using HYSPLIT and compared the results with wind roses obtained from measurements for the analyzed date. The wind roses allowed to know historically the predominance of winds throughout the period 2014-2016 and to distinguish characteristic patterns of pollutant dispersion "wind up" and "wind down" of the Metropolitan Area of Monterrey (MMA). The modeling results showed the predominance of winds, finding that winds at the regional level blow from the east and southeast to the northwest. Therefore, it can be assumed that the emissions generated in Cadereyta and the center of the MMA are transported towards the municipality of García [5].

In the research Analysis of Long-Range Transport Effects on $PM_{2.5}$ during a Short Severe Haze in Beijing, China. Used the HYSPLIT model to study the spatio-temporal variation, long-range transport and potential source regions of $PM_{2.5}$ in Beijing, China and analyzed airflows at different altitudes (500 m,1500 m and 3000 m) in which they obtained that the airflows at 500 m had higher contribution of air pollution and the potential pollution sources were mainly from the northwest Beijing desert and Jing-Jin-Ji (Beijing, Tianjin and Hebei (**Ji**) large cities) built-up areas [6].

The study "PIXE and XRF analysis of atmospheric aerosols from a site in the West

area of Mexico City", used the EPA UNMIX code to determine the number of possible influential pollutant sources, which were then identified by inverse path simulations with HYSPLIT modeling software. In the coarse fraction, four sources were found (mostly soil-related), while the fine fraction had three main sources (fuel, industry and biomass burning). In the study period analysed, the back-trajectories were mostly from the west, with some contributions from the southwest and northwest [1].

Ramirez, in his research Origin of air masses in four cities of Colombia using the HYSPLIT model, identified the origins of air masses in the cities of Bogotá, Cartagena de Indias, Pasto and Leticia, which have the potential to affect urban air quality by transporting particulate matter over long distances from different geographical points. He measured back-trajectories for a period of analysis of one year with heights of 750, 1500 and 2500 m, measured from ground level. He obtained that the most frequent origin of air masses in Cartagena de Indias during 2012 was Caribbean (45%), followed by Continental (36%). In Bogotá it was Continental (77%), followed by East Atlantic (19%). In Pasto it was Pacific (72%), followed by Continental (23%). And in Leticia it was Continental (99%) followed by East Atlantic (1%) [7].

Within the framework of these studies the need arises to know where the pollutants come from and for this there is a valuable research tool known as the HYSPLIT model (Hybrid Single Particle Lagrangian Integrated Trajectory Model) of the Air Resources Laboratory (ARL) of the National Oceanic and Atmospheric Administration (NOAA). This is a complete system for calculating simple air packet trajectories, as well as complex transport, dispersion, chemical transformation, and deposition simulations. HYSPLIT remains one of the most widely used atmospheric dispersion and transport models in the atmospheric science community. One of the most common applications of the model is a reverse trajectory analysis to determine the origin of air masses and to establish source-receptor relationships. HYSPLIT has also been used in a variety of simulations describing the atmospheric transport, dispersion and deposition of pollutants and hazardous materials. Examples of applications include monitoring and forecasting the release of radioactive material [8-10], wildfire smoke [11], windblown dust [12,13], pollutants from various stationary and mobile emission sources [14], allergens [15], and volcanic ash [16].

The scientific foundation and inspiration for HYSPLIT's trajectory capabilities can be traced back to 1949, when the Special Project Section (SPS) (ARL's predecessor) of the U.S. Weather Bureau [now NOAA's National Weather Service (NWS)] was charged with trying to find the source of radioactive debris originating from the first Soviet atomic test and detected by a reconnaissance aircraft near the Kamchatka Peninsula. For that purpose, back trajectories were calculated by hand based on wind data derived from twice-daily radiosonde balloon measurements. These trajectories followed 500-hPa heights assuming geostrophic wind flow. Although these back trajectories were calculated more than 60 years ago, the percentage error between the calculated and actual source location relative to the distance covered by the trajectories was remarkably low about 5% [17]. Since then, trajectory calculations have been one of the backbones of ARL's research activities [18-21].

Many upgrades that reflect the most recent advances in the computation of dispersion and transport have been incorporated into HYSPLIT over the last 15 years. Only a brief introduction is given here; further details can be found in the online supplement. The computation of the new position at a time step (t + ∆t) due to the mean advection by the wind determines the trajectory that a particle or puff will follow. In other words, the change in the position vector P_{mean} with time

$$P_{mean}(t+\Delta t) = P_{mean}(t) + \frac{1}{2}[V(P_{mean}, t) + V(\{P_{mean}(t) + [V(P_{mean}, t)\Delta t]\}, t+\Delta t)]\Delta t \quad (1)$$

is computed from the average of the three-dimensional velocity vectors $\boldsymbol{V}$ at their initial and first-guess positions [22]. Equation (1) is the basis for the calculation of trajectories in HYSPLIT. Only the advection component is considered when running trajectories. The turbulent dispersion component is only needed to describe the atmospheric transport and mixing processes for 3D particles and puffs [21].

The dispersion equations are formulated in terms of the turbulent velocity components. In the 3D particle implementation of the model, the dispersion process is represented by adding a turbulent component to the mean velocity obtained from the meteorological data [23]; namely,

$$X_{final}(t+\Delta t) = X_{mean}(t+\Delta t) + U'(t+\Delta t)\,\Delta t \text{and} \quad (2)$$

$$Z_{final}(t+\Delta t) = Z_{mean}(t+\Delta t) + W'(t+\Delta t)\,\Delta t, \quad (3)$$

where U ' and W ' correspond to the turbulent velocity components, X_{mean} and Z_{mean} are the mean components of the particle positions, and X_{final} and Z_{final} are the final positions in the horizontal and vertical, respectively. The turbulence component is always added after the advection computation.

Here, U ' and W ' are calculated based on the modified discrete-time Langevin equation, which is expressed as a function of the velocity variance, a statistical quantity derived from the meteorological data, and the Lagrangian time scale [21].

This work describes the behavior of the plots in the atmosphere of the Metropolitan Zone of Toluca Valley (MZTV), using the HYSPLIT model. This study has not been carried out to date in the area.

2. MATERIALS AND METHODS

For the study of the movement of the air parcels circulating in the atmosphere of the MZTV, the following methodology was followed:

2.1 Study Sites

Two sites in the MZTV were selected for this study, these were chosen because in previous works they were the sites with the highest concentration of pollutants such as gravimetric, elemental chemical composition, bacteria, fungi and Polycyclic Aromatic Hydrocarbons of $PM_{2.5}$. It is also required to know where the pollutants collected during the campaign come from. The selected sites were San Mateo Atenco (SM) and San Lorenzo Tepaltitlán (SL).

SM is located at Riva Palacio No. 117, Col. Álvaro Obregón. Its geographic coordinates are North Latitude: 19.285455, West Longitude: -99.560438. SM has a territorial area of 21 km^2 with a population density of 4642.6 hab/km^2 [24] and has a total population of 97,418 inhabitants [25]. The climate that characterizes the municipality is temperate semi-warm, sub-humid, long summer and winter rain. Temperatures range from up to minus 5°C and a maximum of 34°C. It has a predominant altitude of 2570 meters above sea level and the average precipitation is 734.10 mm. It has two types of soil: Haplic Feozem (dark surface layer, rich in organic matter and nutrients, suitable for agricultural activities) and Histosol eutrico (soils of lacustrine origin, and extremely rich in organic matter) [26].

SL is a locality of the municipality of Toluca, in the State of Mexico, its geographic coordinates are: North Latitude: 19.317184, West Longitude: -99.621533. SL has an area of about 110 hectares with a population density of 2,133.5 hab/km^2 [23] and has a total population of 35,292 inhabitants [24]. The predominant climate type of SL is temperate, and its temperature is between 12°C and 18°C, this climate is mesothermal and is stable. It has a predominant altitude of 2500 meters above sea level and an average rainfall of 800 mm. Its soil type is Feozem (fertile soil of dark color, rich in organic matter) [27].

2.2 Calculation of Trajectories

The analysis of the backward trajectory model (Backward) consists of analyzing the historical path of the air currents during the 24 h before the day and hour of the selected study, this allows to know the origin of the pollutants, natural or anthropogenic, suspended in the air such as $PM_{2.5}$, among others.

For the selected sites, the calculation of trajectories (Backward) was made for the days 29 June to 8 July. Considering for each day the summertime, central time, relating it to its Coordinated Universal Time (UTC), 00 h (5 UTC), 03 h (8 UTC), 07 h (12 UTC), 12 h (17 UTC), 15 h (20 UTC), 18 h (23 UTC), 19 h (00 UTC) and 22 h (3 UTC).

The movement of the air parcels in the atmosphere of the sites was studied using the HYSPLIT model, under the following procedure [28]:

1. Access the Air Resources Laboratory site: https://www.ready.noaa.gov/HYSPLIT.php
2. The HYSPLIT trajectory model is run.
3. Enter to calculate the file trajectories
4. Path type is selected
5. The meteorological database is chosen, and the geographical coordinates of the sites are inserted

6. The file of the meteorological data of the days to be analyzed is selected
7. On the model execution details page, the parameters are selected according to the requirements to be studied.
8. The site map with the corresponding trajectories is obtained.

2.3 Van de Graff Tandem Particle Accelerator

Within atomic-nuclear energy there is a fundamental tool for its application, the 12 MV Particle Accelerator. With this it is possible to apply different techniques, among which is PIXE (Proton Induced X-Ray Emission) [1,2]. A highly sensitive, multi-elemental and non-destructive technique, with which the elemental chemical concentration present in $PM_{2.5}$ was determined, using a proton beam of 2.5 MeV, a current of 10 A, which deposited a charge on the samples of 4 C, samples taken in the sampling campaign in the period from November 2016 to March 2018.

3. RESULTS AND DISCUSSION

3.1 Study Sites

Fig. 1 shows the sites selected for the study of the movement of air parcels in the atmosphere of the MZTV.

For the SM site (North Lat.: 19.285455, West Long.: -99.560438) trajectories were recorded in the same way as for SL (North Lat.: 19.317184, West Long.: -99.621533), from July 29 to July 8, considering the same schedules. The approximate distance between these two research sites is 8 km, the results are presented below, day by day (Fig. 2 - 11).

3.2 Determination of Trajectories

The methodology described above was followed to determine the trajectories [28]:

1. The URL was entered: **Air Resources Laboratory: https://www.ready.noaa.gov/HYSPLIT.php**
2. **The HYSPLIT trajectory model** was run.
3. **File trajectories** were calculated
4. Type of trajectory was selected:
   a) **The trajectory number was chosen: 1**
   b) **Type of trajectory: Normal**
5. The meteorological database was chosen:
   a) **GDAS(1 grade, global, 2006-present)**
   b) **The geographical coordinates of the sites SM (North Lat.: 19.285455, West Long.: -99.560438) and SL (North Lat.: 19.317184, West Long.: -99.621533) were inserted.**
6. The archive of meteorological data for the days analyzed was selected: **gdas1.jun21.w5**; **gdas1.jul21.w1** and **current7day** (corresponding to June 29 to July 8).
7. In the model execution details page the parameters were selected according to the requirements to be studied:

a) The direction of trajectory selected was Backward
b) Vertical Motion: Vertical velocity model
c) UTC start time: Each day was analyzed at daylight saving time, central time, 00 h (5 UTC), 03 h (8 UTC), 07 h (12 UTC), 12 h (17 UTC), 15 h (20 UTC), 18 h (23 UTC), 19 h (00 UTC) and 22 h (3 UTC).
d) A total execution time of 24 hours
e) Initiated a new trajectory every hour
f) Maximum number of trajectories: 3
g) Previously selected geographic coordinates are automatically displayed here.
h) Automatic height of the middle boundary layer: No
i) Height level 1: 500 meters AGL
j) Display options: Google Earth (kmz)
k) Trajectory requested

8. The site map with the corresponding trajectories is obtained

Trajectories per day were determined for each of the following hours: 00 h (5 UTC), 03 h (8 UTC), 07 h (12 UTC), 12 h (17 UTC), 15 h (20 UTC), 18 h (23 UTC), 19 h (00 UTC) and 22 h (3 UTC). With the results obtained, the behavior between SM and SL was analyzed for each day, considering the different hours.

Fig. 2 shows the backward trajectories (24 h) of the SM and SL site, performed on June 29 with 8 records per day.

Fig. 1. Study sites of San Mateo Atenco (SM) and San Lorenzo (SL)

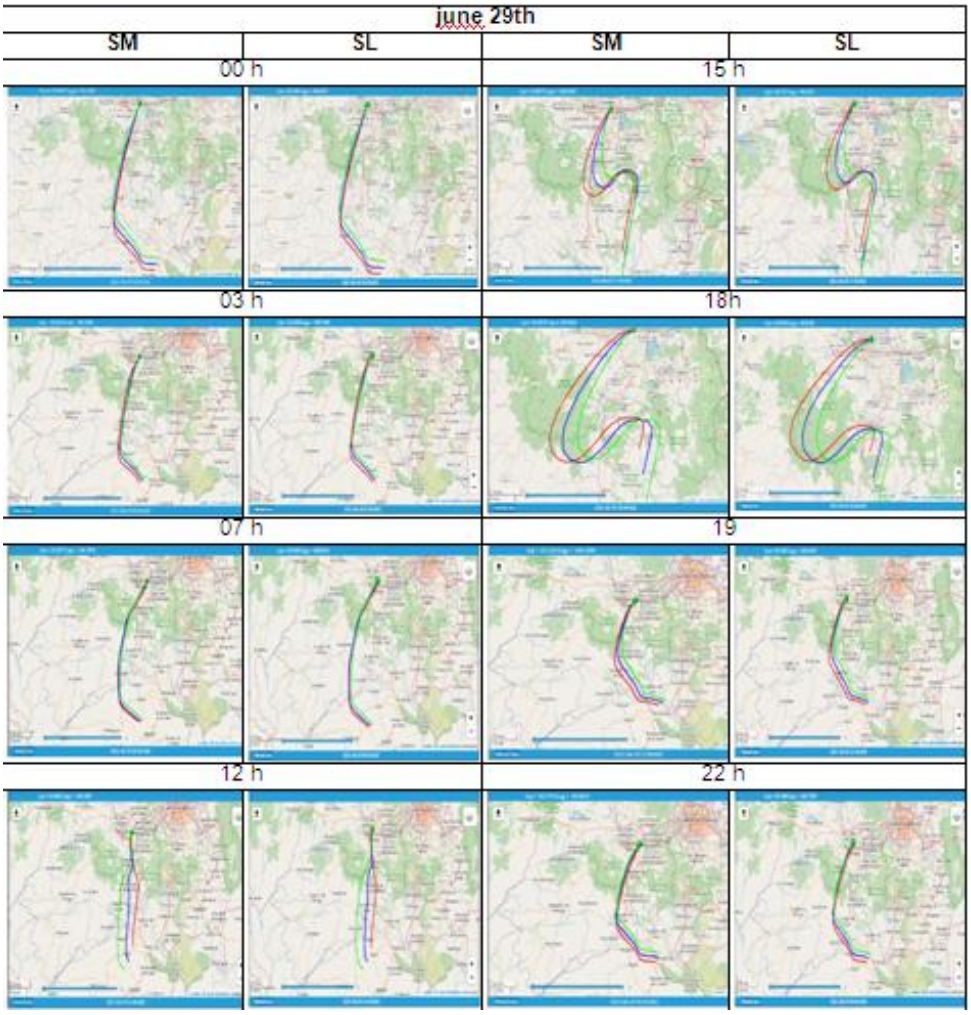

Fig. 2. Backward trajectories of June 29 of the SM and SL sites, from 00 to 22 h [28]

Fig. 2 corresponds to June 29, showing that from 00 h to 12 h, the behavior of the trajectories was similar and came from the southwest. From 15 to 18 h, there were variable changes in direction with respect to the previous one. The 19 and 22 h maintained similar behavior to that of 00 to 12 h. In all cases the two sites showed the same behavior.

Fig. 3 shows the backward trajectories (24 h) of the SM and SL site, performed on June 30 with 8 records per day.

Fig. 3, which corresponds to June 30, showed the following behavior: from 00 h to 07 h, the behavior of the trajectories was similar, and they came from the south. From 12 to 18 h, there were variable changes in direction with respect to the previous one, coming from the north. The 19 and 22 h maintained a similar behavior to that of 00 to 07 h. In all cases, the two sites showed the same behavior.

shows the backward trajectories (24 h) of the SM and SL site. Eight records were taken during June 29 of the present year.

Fig. 4 shows the backward trajectories (24 h) of the SM and SL site, performed on July 1 with 8 records per day.

On July 1, Fig. 4, from 00 h to 12 h, the trajectories of the air parcels were similar to each other, coming from the north and northeast. From 15 to 19 h they had variable changes in direction with respect to the previous one, with a northeasterly direction. The 22 h maintained similar behavior to that of 00 to 03 h. In all cases, the two sites showed the same behavior.

Fig. 5 shows the backward trajectories (24 h) of the SM and SL site, performed on July 2 with 8 records per day.

From Fig. 5, we observe that on July 2 from 00 h to 03 h, the trajectories of the air parcels were similar to each other, coming from the northeast. From 07 h to 18 h they had variable changes in direction with respect to the previous one. The 19 and 22 h maintained similar behavior to that from 00 to 03 h. In all cases, the two sites showed the same behavior.

Fig. 6 shows the backward trajectories (24 h) of the SM and SL site, performed on July 3 with 8 records per day.

On July 3, Fig. 6, from 00 h to 15 h, the trajectories of the air parcels are similar to each other, coming from the southeast. From 18 h and 19 h they have variable changes of direction with respect to the previous ones. The 22 h maintains similar behavior as that of the 00 h. For all the cases, the two sites present the same behavior.

Fig. 7 shows the backward trajectories (24 h) of the SM and SL site, performed on July 4 with 8 records per day.

Fig. 7 shows that on July 4, from 00 h to 12 h, the trajectories of the air parcels were similar to each other, coming from the southeast. The 15 h and 18 h had variable changes in direction with respect to the previous ones. The 19 and 22 h maintained similar behavior to that from 00 to 12 h. In all cases, the two sites showed the same behavior.

Fig. 8 shows the backward trajectories (24 h) of the SM and SL site, performed on July 5 with 8 records per day.

On July 5, Fig. 8, from 00 h to 03 h, the trajectories of the air parcels were similar to each other, coming from the east. From 07 h to 12 h the directions were similar and came from the southwest. The 15 h and 18 h had variable changes in direction with respect to the previous ones. The 19 and 22 h maintained similar behavior to that of the 00 and 03 h. In all cases, the two sites presented the same behavior.

Fig. 9 shows the backward trajectories (24 h) of the SM and SL site, performed on July 6 with 8 records per day.

Fig. 9 shows the results for July 6: From 00 h to 07 h, the trajectories of the air parcels were similar between them, coming from the north. From 12 and 15 h the directions were similar and came from the north. The 18 h and 19 h had variable changes in the direction with respect to the previous ones. At 22 h the behavior was similar to that of 00 h. In all cases, the two sites showed the same behavior.

Fig. 10 shows the backward trajectories (24 h) of the SM and SL site, performed on July 7 with 8 records per day.

Fig. 10 shows the results for July 7: From 00 h to 07 h, the trajectories of the air parcels were similar to each other, coming from the northwest. From 12 h to 19 h they had variable changes of

direction with respect to the previous ones. The 22 h maintained similar behavior to that of 00 h. In all cases, the two sites showed the same behavior.

Fig. 11 shows the backward trajectories (24 h) of the SM and SL site, performed on July 8 with 8 records per day.

Fig. 11 shows the results for July 8: From 00 h to 07 h, the trajectories of the air parcels were similar to each other, coming from the northwest. From 12 h to 18 h they had variable changes in direction with respect to the previous ones. The 19 and 22 h maintained similar behavior to that of the 00 h. In all cases, the two sites showed the same behavior.

Comparing the results of both sites, it was obtained that there is no significant difference, so it was determined that both SM and SL had similarity in the trajectories of the air parcels arriving to them. For this reason, the results indicated for the origins of the backward trajectories (Backward) of the SM site were the same for SL, from June 29 to July 8, at the same times: 00 h (5 UTC), 03 h (8 UTC), 07 h (12 UTC), 12 h (17 UTC), 15 h (20 UTC), 18 h (23 UTC), 19 h (00 UTC) and 22 h (3 UTC).

According to the results obtained for the origins of the trajectories of the air plots, it was observed that in general the origin of the trajectories for both sites was predominantly from the southeast, a situation that is confirmed by the wind roses presented in Fig. 12.

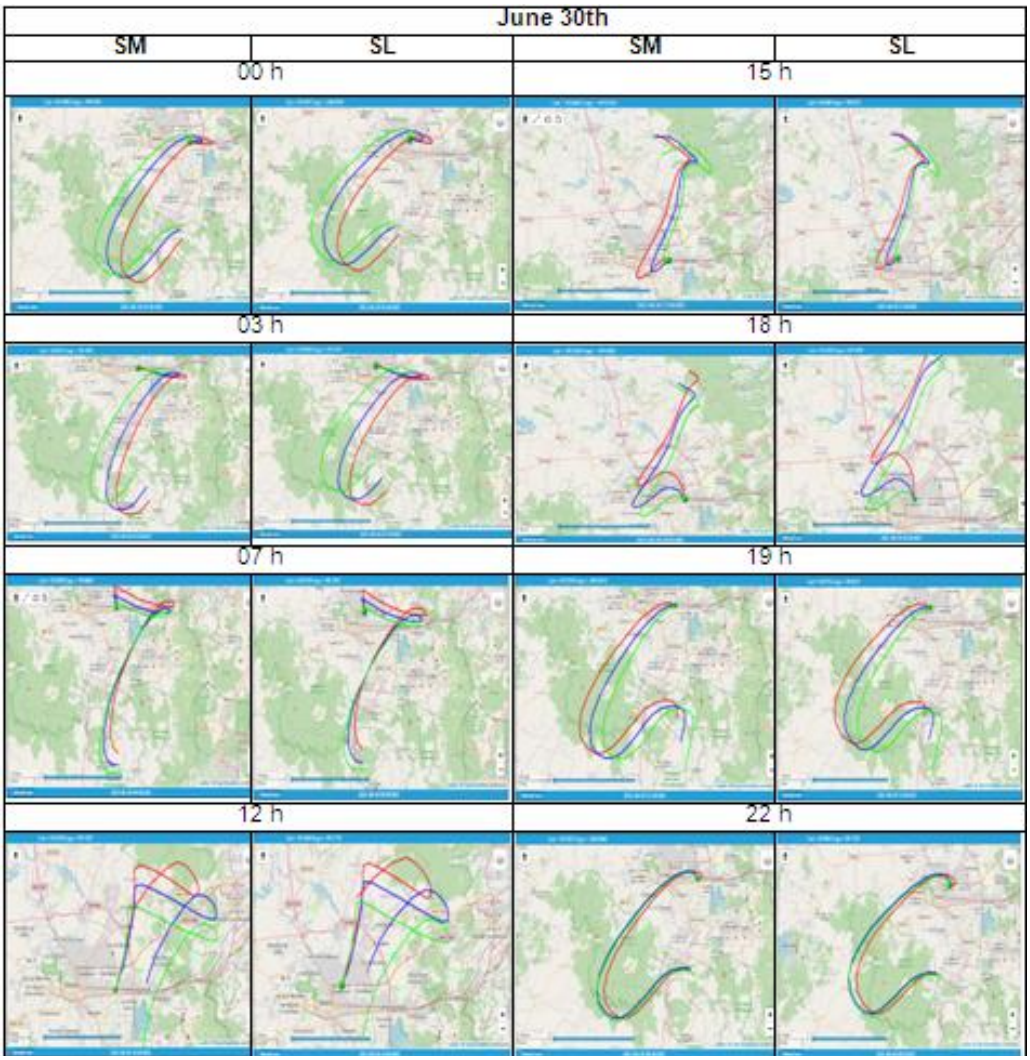

Fig. 3. Backward trajectories of June 30 of the SM and SL sites, from 00 to 22 h [28]

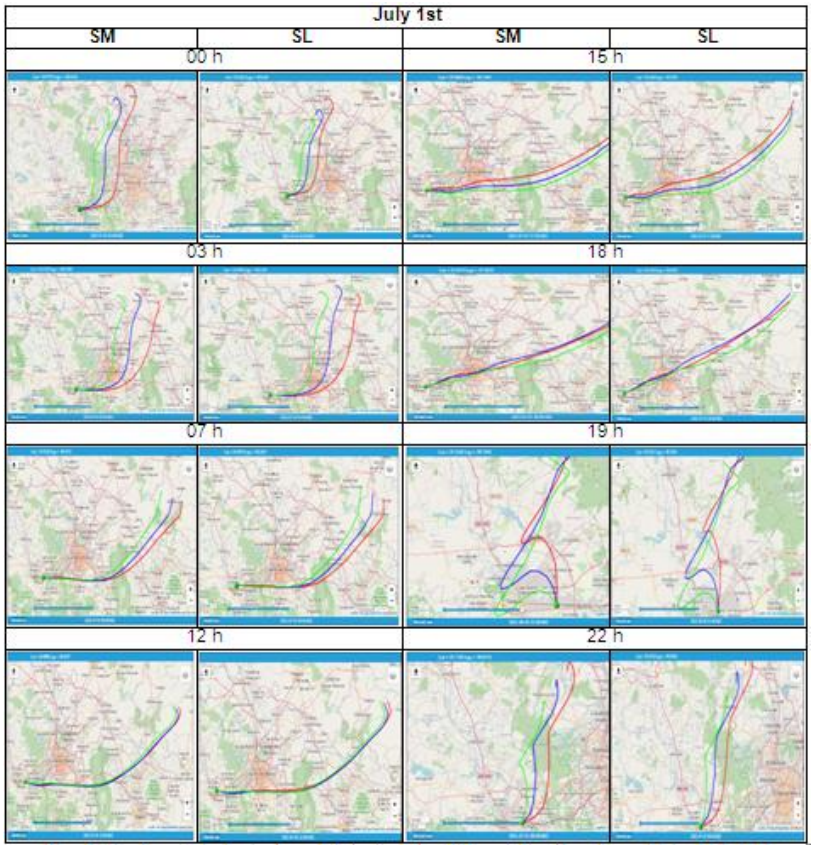

Fig. 4. Backward trajectories of July 1 of the SM and SL sites, from 00 to 22 h [28]

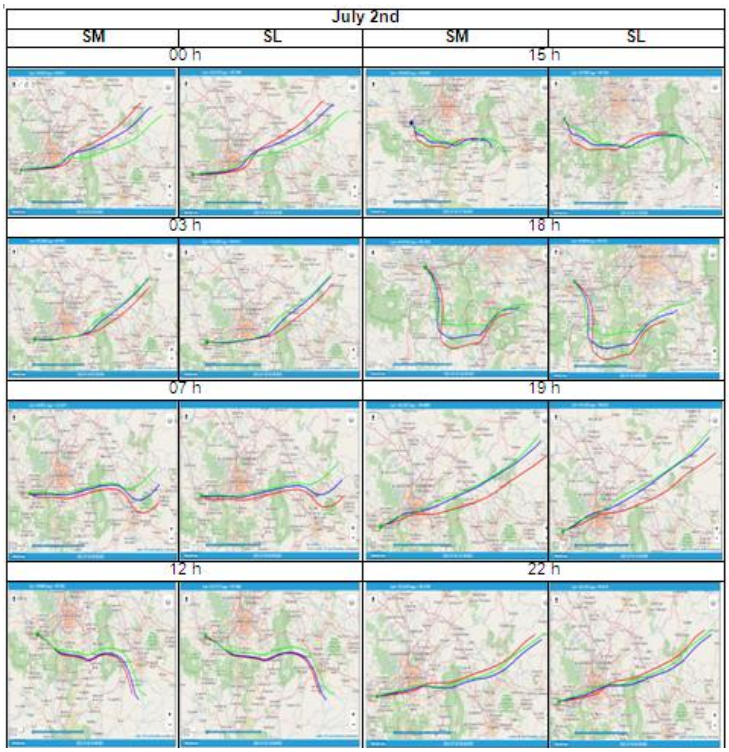

Fig. 5. Backward trajectories of July 2 of the SM and SL sites, from 00 to 22 h [28]

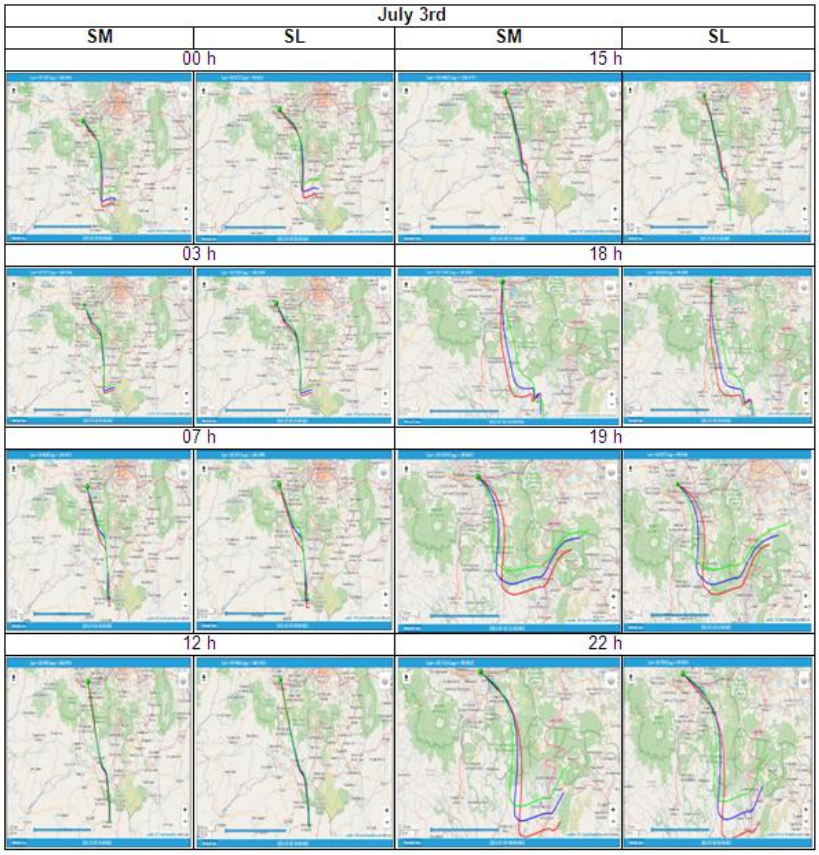

Fig. 6. Backward trajectories of July 3 of the SM and SL sites, from 00 to 22 h [28]

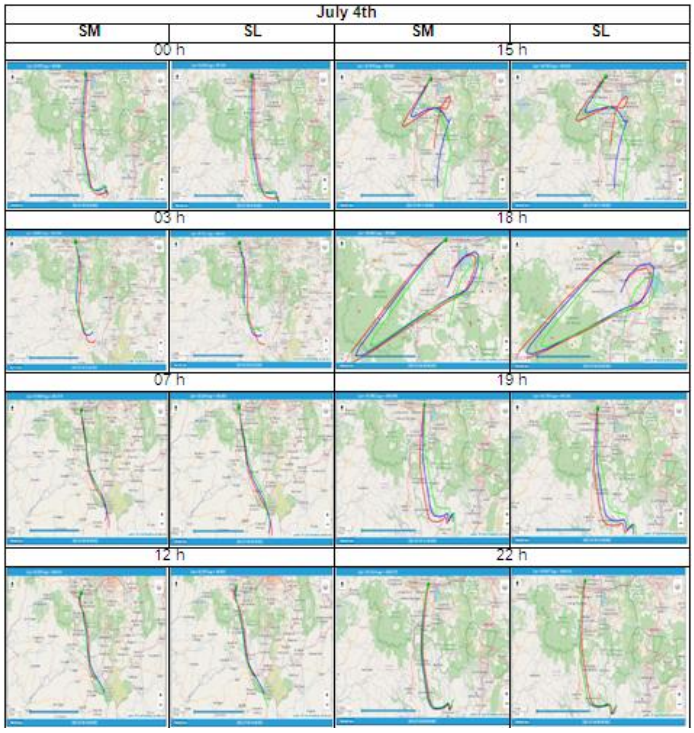

Fig. 7 Backward trajectories of July 4 of the SM and SL sites, from 00 to 22 h [28]

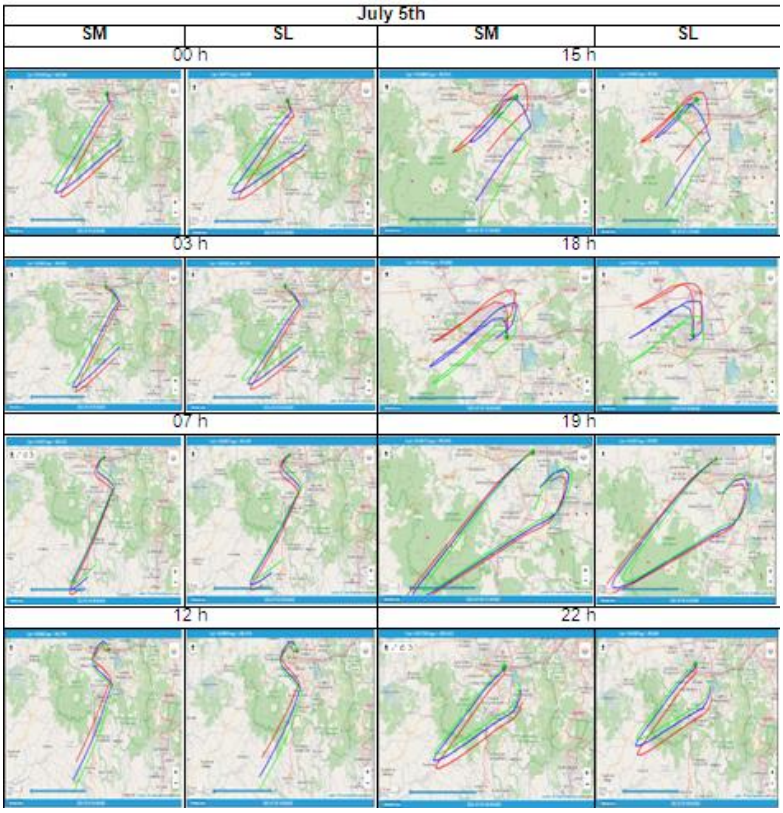

Fig. 8 Backward trajectories of July 5 of the SM and SL sites, from 00 to 22 h [28]

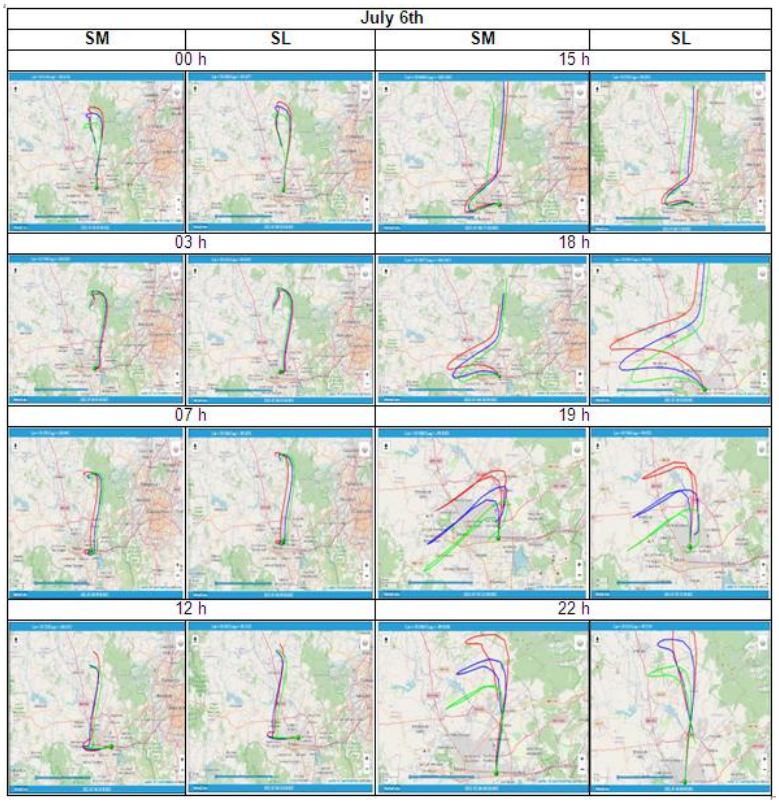

Fig. 9. Backward trajectories of July 6 of the SM and SL sites, from 00 to 22 h [28]

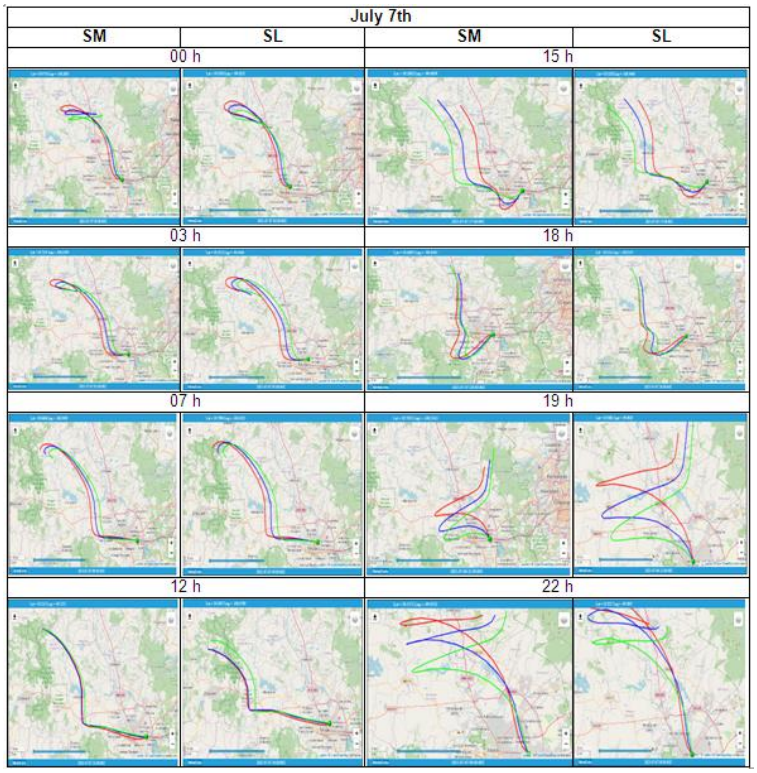

Fig. 10. Backward trajectories of July 7 of the SM and SL sites, from 00 to 22 h [28]

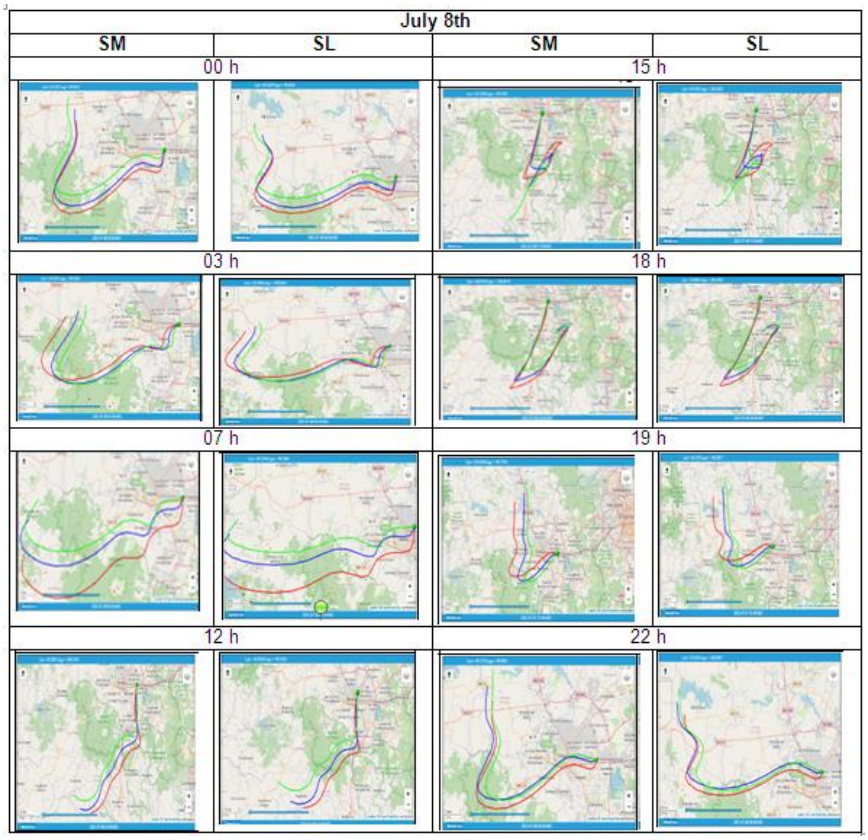

Fig. 11. Backward trajectories of July 8 of the SM and SL sites, from 00 to 22 h [28]

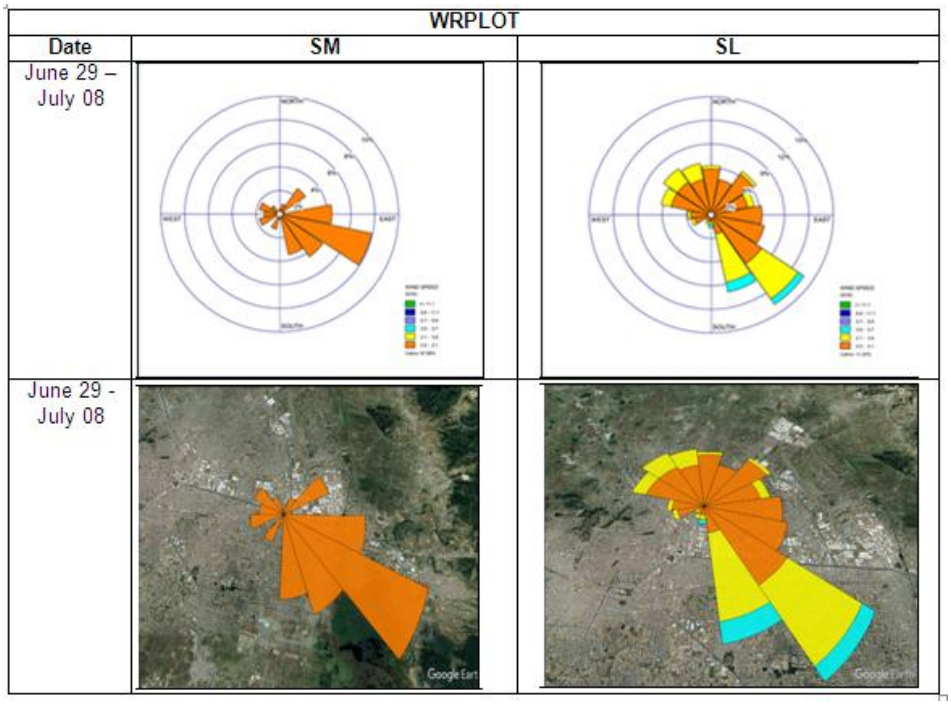

Fig. 12. Wind rose (blowing from) from 29 June to 08 Jul of the SM and SL sites [29]

Considering the results obtained for the trajectories and the wind rose, it is observed that the plots influence in the same way at least in both sites of this study. To corroborate these results, taking advantage of the concentrations of the elemental chemical composition of $PM_{2.5}$ obtained through the application of the PIXE (Proton Induced X-Ray Emission) technique to the samples taken in a sampling campaign in six sites of the MZTV from November 2016 to March 2018, an ANOVA analysis (with a significance level of α=0.05) was performed for the concentrations of SM and SL with the objective of seeing the equality of their behavior. The results in this regard were: for sulfur (p=0.060468), chlorine (p=0.261553), potassium (p=0.254962), titanium (p=0.209594), vanadium (p= 0. 752732), chromium (p=0.191684), manganese (p=0.305537), nickel (p= 0.340482), copper (p=0.569438), zinc (p=0.271316) and lead (p=0.318787). Since the p-value is in all cases is greater than the significance level of 0.05, the null hypothesis is accepted, and it is possible to conclude that the elemental chemical composition of $PM_{2.5}$ have equal means in both sites (SM and SL).

4. CONCLUSION

HYSPLIT is one of the most used models for the study of the dispersion and trajectories of pollutants; with them it is possible to know their possible sources of emission. Using this model, we determined the possible origins of the contaminants that reach San Mateo Atenco and San Lorenzo, in the Metropolitan Zone of the Toluca Valley. From the results it was observed that the behavior of the trajectories of the air parcels at both sites is similar. It is observed that the trajectories for the same day are the same at both sites but different for another day. It was determined that during the night-day (19 to 12 h of the following day), the behavior is similar and changes during the remaining time, being variable. With the results of this work, it is possible to consider the behavior of meteorological parameters and thus take them into account for sampling studies of criteria pollutants such as $PM_{2.5}$. The wind roses generated confirmed the direction of the air trajectories arriving at the study sites. From the results obtained, it is important to highlight that the contaminants arriving at one site are similar to those arriving at the other study site, at least for the SM and SL sites. Although there is a possibility that the same thing is happening in the whole area, a situation that should be corroborated with more studies. In addition, in the MZTV the buildings are not very high, which avoids the existence of microclimates.

CONSENT (WHERE EVER APPLICABLE)

It is not applicable.

ETHICAL APPROVAL (WHERE EVER APPLICABLE)

It is not applicable.

ACKNOWLEDGEMENTS

The authors would like to express their gratitude to the following organizations: to the secretaria de educación pública-consejo nacional de ciencia y tecnología (sep-conacyt) for funding for the execution of project cb:2015-01-256751; to national institute for nuclear research for the support to this research.

COMPETING INTERESTS

Authors have declared that no competing interests exist.

REFERENCES

1. Díaz RV, López-Monroy J, Miranda J, Espinosa AA. PIXE and XRF analysis of atmospheric aerosols from a site in the West area of Mexico City. Nuclear Instruments and Methods in Physics Research Section B: Beam Interactions with Materials and Atoms. 2014;318:Part A: 135-138. Avaailable:https://doi.org/10.1016/j.nimb.2013.05.095
2. Díaz-Godoy RV, López-Monroy J, Moreno-Alcántara J, Castellanos-Moguel J, Nuñez-Cardona MT, Sierra-Vargas MP, Aztatzi-Aguilar OG, Flores-Ortiz A. Spatial Evaluation of Health Risk due to Inhalation of $PM_{2.5}$ Pollutants in the Metropolitan Areas of Toluca Valley and Mexico Valley. Journal of Energy Research and Reviews. 2021; 8(3), 1-16. Avaialable:https://doi.org/10.9734/jenrr/2021/v8i330210
3. Ortínez-Álvarez A, Ruiz-Suárez LG. Ortega E, García-Reynoso A, Peralta O, López-Gaona A, Castro T, Martínez-Arroyo A. Emission inventory point source source visualization on Google Earth and integrated with HYSPLIT model. Atmósfera. 2021; 34(2), 143-156. Avaialble:https://doi.org/10.20937/ATM.52834
4. Lee D, Choi JY, Myoung J, Kim O, Park J, Shin HJ, Ban SJ, Park HJ, Nam KP. Analysis of a Severe $PM_{2.5}$ Episode in the Seoul Metropolitan Area in South Korea from 27 February to 7 March 2019: Focused on Estimation of Domestic and Foreign Contribution. Atmosphere. 2019;10(12):756. Abaialble:https://doi.org/10.3390/atmos10120756
5. Molina M, Mena C, Meviavilla-Sahagún A, Gómez-Sánchez MD, Barrera-Huertas HA, García-Escalante J, Hernández-Valdez N, CONACYT et al. (2019). Analysis of $PM_{2.5}$ pollution in the city of Monterrey, Nuevo León, focused on the identification of strategic control measures, Centro Mario Molina para estudios estratégicos sobre energía y medio ambiente A. C; 2019. [online]. Available:http://aire.nl.gob.mx/docs/reportes/An%C3%A1lisis_de_la_Contaminaci%C3%B3n_PM2_5_Monterrey.pdf 02/08/2021
6. Yang W, Wang G, Bi C. Analysis of Long-Range Transport Effects on $PM_{2.5}$ during a Short Severe Haze in Beijing, China. Aerosol Air Qual. Res. 2017; 17(6): 1610-1622. Avaialble:https://doi.org/10.4209/aaqr.2016.06.0220.
7. Ramírez-Hernández O. J. Origin of air masses in four cities of Colombia using the HYSPLIT model. RIAA. 2014;5(1): 103-119. Avaialble:https://doi.org/10.22490/21456453.935
8. Connan O, Smith K, Organo C, Solier L, Maro D, Hébert D. Comparison of RIMPUFF, HYSPLIT, ADMS atmospheric dispersion model outputs, using emergency response procedures, with 85Kr measurements made in the vicinity of nuclear reprocessing plant. J. Environ. Radioact. 2013; 124, 266-277. Available:https://doi.org/10.1016/j.jenvrad.2013.06.004
9. Bowyer TW, Kephart R, Eslinger PW, Friese JI, Miley HS, Saey PRJ. Maximum reasonable radioxenon releases from medical isotope production facilities and their effect on monitoring nuclear explosions. J. Environ. Radioact. 2013;115:192-200. Available:https://doi.org/10.1016/j.jenvrad.2012.07.018.
10. Jeong H, Park M, Jeong H, Hwang W, Kim E, Han M. Radiological risk assessment

caused by RDD terrorism in an urban area. Appl. Radiat. Isot. 2013;79:1-4. Available:https://doi.org/10.1016/j.apradiso.2013.04.018

11. Rolph GD, Draxler RR, Stein AF, Taylor A, Ruminski MG, Kondragunta S, Zeng J, Huang H, Manikin G, McQueen JT, Davidson PM. Description and Verification of the NOAA Smoke Forecasting System: The 2007 Fire Season. Weather and Forecasting. 2009;24(2):361-378. Available:https://doi.org/10.1175/2008WAF2222165.1.
12. Escudero MA, Stein A, Draxler RR, Querol X, Alastuey A, Castillo S, Avila A. Determination of the contribution of northern Africa dust source areas to PM_{10} concentrations over the central Iberian Peninsula using the Hybrid Single-Particle Lagrangian Integrated Trajectory model (HYSPLIT) model. J. Geophys. Res. 2006; 111 (D6210). Available:https://doi.org/10.1029/2005JD006395
13. Gaiero DM, Simonella L, Gassó S, Gili AF, Stein P, Sosa R, Becchio R, Arce J, Marelli H. Ground/satellite observations and atmospheric modeling of dust storms originated in the high Puna-Altiplano deserts (South America): Implications for the interpretation of paleo-climatic archives. J. Geophys. Res. 2013; 118 (9): 3817-3831. Available:https://doi.org/10.1002/jgrd.50036
14. Chen B, Stein AF, Castell N, de la Rosa JD, Sánchez de la Campa AM. González-Castanedo Y. and Draxler R. R. Modeling and surface observations of arsenic dispersion from a large Cu-smelter in southwestern Europe. Atmos. Environ. 2012;49:114-122, Avaialble:https://doi.org/10.1016/j.atmosenv.2011.12.014
15. Efstathiou C, Isukapalli S, Georgopoulos P. A mechanistic modeling system for estimating large-scale emissions and transport of pollen and co-allergens. Atmos. Environ. 2011;45(13):2260-2276. Avaialble:https://doi.org/10.1016/j.atmosenv.2010.12.008
16. Stunder BJB. An Assessment of the Quality of Forecast Trajectories. J. Appl. Meteor. 1996;35(8):1319-1331. Avaialble:https://doi.org/10.1175/1520-0450(1996)035<1319:AAOTQO>2.0.CO;2
17. Machta L. Finding the site of the first Soviet nuclear test in 1949. Bull. Amer. Meteor. Soc. 1992;73(11):1797-1806. Avaialble:https://doi.org/10.1175/1520-0477(1992)073<1797:FTSOTF>2.0.CO;2
18. Angell JK, Pack DH, Holzworth GC, Dickson CR. Tetroon Trajectories in an Urban Atmosphere. Journal of Applied Meteorology and Climatology. 1966;5(5): 565-572. Avaialble:https://doi.org/10.1175/1520-0450(1966)005<0565:TTIAUA>2.0.CO;2
19. Angell JK, Pack DH, Machta L, Dickson CR, Hoecker WH. Three-Dimensional Air Trajectories Determined from Tetroon Flights in the Planetary Boundary Layer of the Los Angeles Basin. Journal of Applied Meteorology and Climatology. 1972;11(3):451-471. Avaialble:https://doi.org/10.1175/1520-0450(1972)011<0451:TDATDF>2.0.CO;2
20. Angell JK, Dickson CR, Hoecker Jr WH, Tetroon Trajectories in the Los Angeles Basin Defining the Source of Air Reaching the San Bernardino-Riverside Area in Late Afternoon. Journal of Applied Meteorology and Climatology. 1976;15(3):197-204. Avaialble:https://doi.org/10.1175/1520-0450(1976)015<0197:TTITLA>2.0.CO;2
21. Stein AF, Draxler RR, Rolph GD, Stunder BJB, Cohen MD, Ngan F. NOAA's HYSPLIT Atmospheric Transport and Dispersion Modeling System. BAMS. 2015;96 (12):2059-2077. Avaialble:https://doi.org/10.1175/BAMS-D-14-00110.1.
22. Draxler RR, Hess GD. An overview of the HYSPLIT_4 modeling system for trajectories, dispersion, and deposition. Aust. Meteor. Mag. 1998;47(4):295-308. ISSN: 0004-9743. Avaialble:https://www.researchgate.net/publication/235961417_An_overview_of_the_HYSPLIT_4_modeling_system_for_trajectories_dispersion_and_deposition
23. Fay B, Glaab H, Jacobsen I, Schrodin R. Evaluation of Eulerian and Lagrangian atmospheric transport models at the Deutscher Wetterdienst using anatex surface tracer data. Atmos. Environ. 1995; 29 (18):2485-2497. Avaialble:https://doi.org/10.1016/1352-2310(95)00144-N
24. INEGIa. Socio-demographic Panorama of Mexico, Population and Housing Census 2020, National Institute of Statistics and Geography; 2020. [online].

Avaialble:https://inegi.org.mx/contenidos/productos/prod_serv/contenidos/espanol/bvinegi/productos/nueva_estruc/702825197889.pdf 06/08/2021

25. INEGIb. Population and Housing Census 2020, Main results by locality (ITER), National Institute of Statistics and Geography; 2020. [online]. Avaialble:https://www.inegi.org.mx/app/scitel/Default?ev=9 06/08/2021
26. Ipomex. Risk Atlas 2014, H. Ayuntamiento de Toluca. 2015. [online]. Avaiable:https://www.ipomex.org.mx/recursos/ipo/files_ipo/2015/8/6/85a8bfedadcaa7e761f7abe7f29a2db2.pdf 20/08/2021
27. Ipomex. Risk Atlas. H. Ayuntamiento de San Mateo Atenco; 2018. [online]. Avaialble:https://www.ipomex.org.mx/recursos/ipo/files_ipo3/2018/43031/5/561a0af76b9277fd76e6f5adf0377305.pdf 20/08/2021
28. NOAA. HYSPLIT. Air Resources Laboratory; 2021 [online]. Avaialble:https://www.ready.noaa.gov/HYSPLIT.php07/08/2021
29. Lakes Software. WRPLOT view^{TM}, Wind Rose Plots Metereological Data. 2021; version 8.0.2-20.6. Avaialble:https://www.weblakes.com/software/freeware/wrplot-view/

Peer-review history:
The peer review history for this paper can be accessed here:
http://www.sdiarticle4.com/review-history/75258